# Microscopic description of $\alpha$-like resonances

D. S. Delion
*National Institute of Physics and Nuclear Engineering, Bucharest-Măgurele, POB MG-6, Romania*

J. Suhonen
*Department of Physics, University of Jyväskylä, POB 35, FIN-40351 Jyväskylä, Finland*
(Received 12 July 1999; published 4 January 2000)

A description of $\alpha$-like resonances is given in terms of single-particle states including narrow Gamow resonances in continuum. The equations of motion are derived within the multistep shell-model approach; the lowest collective two-particle eigenmodes are used as building blocks for the four-particle states. A good agreement with the low-lying states in $^{212}$Po is obtained. A new technique to estimate the $\alpha$-particle formation amplitude for any multipolarity is proposed. The spectroscopic factor of the $\alpha$-decay between ground states is reproduced, but the total width is by two orders of magnitude less than the experimental total width, due to the absence of the background components. The $\alpha$-like structure of the lowest states in $^{212}$Po is analyzed and strong high-lying resonances are predicted. The derived equivalent local potential for the $\alpha$-particle scattering has a molecular shape.

PACS number(s): 21.60.Cs, 21.60.Gx, 23.60.+e

## I. INTRODUCTION

Although the first paper in theoretical nuclear physics was devoted to the $\alpha$-decay and provided a nice explanation in terms of the Coulomb-barrier penetration of a preformed $\alpha$-particle [1], the microscopic description of the cluster formation on the nuclear surface is still an open problem. The usual shell-model configuration space used in the estimation of the $\alpha$-cluster probability is not able to reproduce the absolute value of the half-life for the transition between the ground states [2]. This deficiency is connected with the asymptotic exponential decrease of the bound single particle (sp) wave functions [3]. An answer to the problem would be the inclusion of the sp narrow resonances lying in continuum [4–6], the so-called Gamow states. In spite of the fact that the true asymptotic behavior of the wave functions is achieved, the value of the half-life is still not reproduced. The inclusion of the background contribution becomes important because an important part of the alpha-clustering process proceeds through such states.

The problem of considering the continuum part of the spectrum in microscopic calculations is rather involved, but very important especially for drip-line nuclei [7]. To estimate the decay width these states can be taken into account effectively by including an $\alpha$-cluster component [8] or by considering a sp basis with a larger harmonic oscillator (ho) parameter for states in continuum [9]. The idea to replace the integration over the real spectrum in continuum by sp Gamow resonances plus an integration along a contour in the complex plane including these resonances was considered by Berggren in Ref. [10]. The calculation is very much simplified if one considers that in some physical processes only the narrow resonances are relevant and the integration, giving the background, can be neglected [11,12]. This was shown to be an adequate approach for instance in giant resonances [13] and in the nucleon decay processes [14].

But narrow sp Gamow resonances can become a useful tool in analyzing the high-lying $\alpha$-like four-particle states which were observed long time ago as resonances in the $\alpha$-particle anomalous large angle scattering (ALAS) and connected with the so called ''quasimolecular states.'' Such states were mainly observed and analyzed in the $\alpha$ scattering on light nuclei like $^{16}$O [15], $^{40}$Ca [16], or $^{28}$Si [17], but it is also interesting to look for such states in heavy nuclei such as $^{208}$Pb [18].

The aim of our paper is to put in evidence that such resonances can be indeed built on top of Gamow sp resonances and they have a similar structure with the low-lying alpha-decaying states. As an example we chose the nucleus $^{212}$Po which exhibits a nice $\alpha$-like structure on top of the double-magic nucleus $^{208}$Pb. The article is organized as follows: in Sec. II we shortly describe the multistep shell-model formalism which is a very appropriate approach for such a structure and the calculation of the formation amplitude of the $\alpha$-clusters. Here we propose a simple and efficient method for the analytical estimation of the overlap integrals in the case of Gamow resonances. In Sec. III we analyze the numerical results concerning both low-lying and high-lying parts of the spectrum and derive an equivalent local potential describing the $\alpha$-particle motion. The conclusions are drawn in the last section.

## II. THEORETICAL BACKGROUND

The analysis of the low-lying spectrum of $^{212}$Po was performed in Ref. [19], where the four-particle equations of motion were written in terms of the two-particle eigenstates. This procedure is related to the so-called multistep shell-model (MSM) procedure [20]. It was used in describing the $^{212}$Po nucleus [21,22] in connection with the microscopic description of the alpha decay between the ground states (g.s.). In the following we will first shortly describe this procedure in order to introduce the essential notations and to compute the formation amplitude of the $\alpha$ cluster for any multipolarity.

 

### A. Two-particle TDA

In order to build a four-particle state let us first introduce the correlated two-particle state of a multipolarity $\alpha_2$

$$|\tau_1\tau_2;\alpha_2 a_2\rangle = P^\dagger_{\alpha_2}(\tau_1\tau_2;a_2)|0\rangle, \tag{2.1}$$

where $\tau$ is the isospin index defining proton-proton ($pp$), neutron-neutron ($nn$) and proton-neutron ($pn$) states in $^{210}$Po, $^{210}$Pb and $^{210}$Bi nuclei, respectively. The two-particle creation operator for correlated pairs defines the $a_2$th eigenstate of the Tamm-Dankoff approach (TDA), which has actually a two-particle shell model ansatz

$$P^\dagger_{\alpha_2}(\tau_1\tau_2;a_2) = \sum_{ij} X_{\tau_1\tau_2}(ij;\alpha_2 a_2) C^\dagger_{\alpha_2}(\tau_1\tau_2;ij). \tag{2.2}$$

Here the summation is taken over all the indices, denoting spherical shell model quantum numbers, $ij$ if $\tau_1 \neq \tau_2$ and over $i \leqslant j$ if $\tau_1 = \tau_2$. The normalized pair operators are defined as

$$C^\dagger_{\alpha_2}(\tau_1\tau_2;ij) = \frac{1}{\Delta_{ij}}[c^\dagger_{\tau_1 i} c^\dagger_{\tau_2 j}]_{\alpha_2}, \quad \Delta_{ij} \equiv \sqrt{1+\delta_{\tau_1\tau_2}\delta_{ij}}, \tag{2.3}$$

where the bracket denotes the angular-momentum coupling. These operators, as well as the correlated ones defined by Eq. (2.2), satisfy the boson commutation rules from which one gets the TDA orthonormality relations for the amplitudes.

The Hamiltonian for a spherical nucleus is written as a superposition of different multipoles in the particle-particle coupling scheme:

$$\begin{aligned} H = & \sum_{\tau j} \epsilon_{\tau j} N_{\tau j} \\ & + \frac{1}{2} \sum_{\alpha_2} \sum_{\tau_1\tau_2} \sum_{i_1 j_1} \sum_{i_2 j_2} \langle \tau_1\tau_2;i_1 j_1;\alpha_2|V|\tau_1\tau_2;i_2 j_2;\alpha_2\rangle \\ & \times C^\dagger_{\alpha_2}(\tau_1\tau_2;i_1 j_1) C_{\alpha_2}(\tau_1\tau_2;i_2 j_2). \end{aligned} \tag{2.4}$$

The equation of motion

$$[H, P^\dagger_{\alpha_2}(\tau_1\tau_2;a_2)] = E_{\alpha_2}(\tau_1\tau_2;a_2) P^\dagger_{\alpha_2}(\tau_1\tau_2;a_2) \tag{2.5}$$

leads to the two-particle TDA system of equations

$$\begin{aligned} & \frac{1}{2} \sum_{kl} \langle \tau_1\tau_2;ij;\alpha_2|V|\tau_1\tau_2;kl;\alpha_2\rangle X_{\tau_1\tau_2}(kl;\alpha_2 a_2) \\ & \quad = [E_{\alpha_2}(\tau_1\tau_2;a_2) - \epsilon_{\tau_1 i} - \epsilon_{\tau_2 j}] X_{\tau_1\tau_2}(ij;\alpha_2 a_2), \end{aligned} \tag{2.6}$$

where $\epsilon_{\tau i}$ is the sp energy of the $i$th spherical level.

### B. Four-particle TDA

The correlated four-particle eigenstate $a_4$ of multipolarity $\alpha_4$ is defined as follows:

$$|\alpha_4 a_4\rangle = P^\dagger_{\alpha_4}(a_4)|0\rangle, \tag{2.7}$$

where the four-particle (quartet) creation operator has two main components:

$$\begin{aligned} P^\dagger_{\alpha_4}(a_4) \equiv & \sum_2 X(pp\alpha_2 a_2; nn\beta_2 b_2; \alpha_4 a_4) \\ & \times [P^\dagger_{\alpha_2}(pp;a_2) P^\dagger_{\beta_2}(nn;b_2)]_{\alpha_4} \\ & + \sum_2 X(pn\alpha_2 a_2; pn\beta_2 b_2; \alpha_4 a_4) \\ & \times [P^\dagger_{\alpha_2}(pn;a_2) P^\dagger_{\beta_2}(pn;b_2)]_{\alpha_4}. \end{aligned} \tag{2.8}$$

For a core state $|0\rangle = |^{208}\mathrm{Pb}\rangle$ these two terms correspond to the couplings $(^{210}\mathrm{Po} \otimes ^{210}\mathrm{Pb})_{\alpha_4 a_4}$ and $(^{210}\mathrm{Bi} \otimes ^{210}\mathrm{Bi})_{\alpha_4 a_4}$, respectively.

By using the short-hand notations $\alpha_2 \equiv (\tau_1\tau_2\alpha_2 a_2)$ and $\alpha_4 \equiv (\alpha_4 a_4)$ the above relation can be written as follows:

$$P^\dagger_{\alpha_4} = \sum_2 X(\alpha_2\beta_2)[P^\dagger_{\alpha_2} P^\dagger_{\beta_2}]_{\alpha_4}. \tag{2.9}$$

Using the TDA equation of motion for the four-particle system

$$[H, P^\dagger_{\alpha_4}] = E_{\alpha_4} P^\dagger_{\alpha_4} \tag{2.10}$$

and the analogous two-particle equation (2.5) one obtains, by using the symmetrized double commutator, the following system of equations:

$$\begin{aligned} & \sum_{2'} H(\alpha_2\beta_2;\alpha'_2\beta'_2) X(\alpha'_2\beta'_2) \\ & \quad = E_{\alpha_4} \sum_{2'} I(\alpha_2\beta_2;\alpha'_2\beta'_2) X(\alpha'_2\beta'_2), \end{aligned} \tag{2.11}$$

where the metric matrix is defined by the following overlap integral:

$$I(\alpha_2\beta_2;\alpha'_2\beta'_2) \equiv \langle 0|P_{\alpha_4}(\alpha_2\beta_2) P^\dagger_{\alpha_4}(\alpha'_2\beta'_2)|0\rangle, \tag{2.12}$$

and the Hamiltonian matrix is proportional to the metric matrix

$$\begin{aligned} H(\alpha_2\beta_2;\alpha'_2\beta'_2) \equiv & \frac{1}{2}\langle 0|[P_{\alpha_4}(\alpha_2\beta_2), H, P^\dagger_{\alpha_4}(\alpha'_2\beta'_2)]|0\rangle \\ = & \frac{1}{2}(E_{\alpha_2} + E_{\beta_2} + E_{\alpha'_2} + E_{\beta'_2}) I(\alpha_2\beta_2;\alpha'_2\beta'_2). \end{aligned} \tag{2.13}$$

The MSM system of equations (2.11) is formally different from Ref. [20] which uses a non-symmetric Hamiltonian matrix, but it can be shown that they are equivalent. The metric matrix elements are computed using the standard angular-momentum recoupling procedure and the final result is given in Appendix A. In such a way the interaction is involved only in the first two-particle step. In the second four-particle step only the two-particle energies enter the equation of motion. The system of equations (2.11) can be solved using as an orthonormal basis the eigenstates of the metric matrix, as described in Appendix B.

### C. $\alpha$-particle formation amplitude

Let us consider the $\alpha$-decay process

$$B \rightarrow A + \alpha. \tag{2.14}$$

The amplitude of this process, called the $\alpha$-particle formation amplitude, is given as an overlap integral over the internal coordinates of the daughter nucleus and the emitted cluster

$$\langle A|B\rangle \equiv \int d\xi_\alpha d\xi_A \psi_\alpha^*(\xi_\alpha)\psi_A^*(\xi_A)\psi_B(\xi_B). \tag{2.15}$$

The modulus squared of this overlap bears the meaning of $\alpha$-cluster probability inside the mother wave function. We will use it to analyze the $\alpha$-like structure of all eigenstates in $^{212}$Po.

The $\alpha$-particle internal wave function is a product of the ho and singlet-spin wave functions [23]

$$\psi_\alpha(\xi_\alpha) \equiv \phi_{00}^{(\lambda_\alpha)}(\vec{r}_\pi)\phi_{00}^{(\lambda_\alpha)}(\vec{r}_\nu)\phi_{00}^{(\lambda_\alpha)}(\vec{r}_\alpha)\chi_{00}^{(\pi)}(12)\chi_{00}^{(\nu)}(34), \tag{2.16}$$

where $\lambda_\alpha \approx 0.5$ fm$^{-2}$ is the $\alpha$-particle ho parameter. These wave functions are written in terms of the relative and center of mass (c.m.) Moshinsky coordinates

$$\begin{pmatrix} \vec{r}_\pi \\ \vec{R}_\pi \end{pmatrix} = \frac{\vec{r}_1 \mp \vec{r}_2}{\sqrt{2}}, \quad \begin{pmatrix} \vec{r}_\nu \\ \vec{R}_\nu \end{pmatrix} = \frac{\vec{r}_3 \mp \vec{r}_4}{\sqrt{2}}, \quad \begin{pmatrix} \vec{r}_\alpha \\ \vec{R}_\alpha \end{pmatrix} = \frac{\vec{R}_\pi \mp \vec{R}_\nu}{\sqrt{2}}. \tag{2.17}$$

The volume elements are connected by

$$d\vec{r}_1 d\vec{r}_2 d\vec{r}_3 d\vec{r}_4 = 8 d\vec{r}_\pi d\vec{r}_\nu d\vec{r}_\alpha d\vec{R}_\alpha \equiv d\vec{\xi}_\alpha d\vec{R}_\alpha. \tag{2.18}$$

The mother wave function, according to the MSM procedure, is a product between the four-particle and the daughter wave functions, i.e.,

$$\psi_B(\xi_B) \equiv \psi_{\alpha_4 a_4}(1234)\psi_A(\xi_A). \tag{2.19}$$

The overlap integral (2.15) then becomes

$$\langle A|B\rangle = \int d\xi_\alpha \psi_\alpha^*(\xi_\alpha)\psi_{\alpha_4 a_4}(1234) = \mathcal{F}_{\alpha_4 a_4}(R_\alpha) Y_{\alpha_4}(\hat{R}_\alpha). \tag{2.20}$$

The integration is performed over the relative coordinates and the result is a function of the $\alpha$-particle c.m. coordinate $\vec{R}_\alpha$. The angular momentum $l = \alpha_4$ for transitions of spherical nuclei is given by the difference between the final and initial spins of the mother and daughter states.

In order to estimate the decay width (proportional to the inverse of the half-life) the function defined by Eq. (2.20) is used as an initial condition to solve a system of differential equations describing the motion of the $\alpha$ particle in the potential of the daughter nucleus. In the case of spherical nuclei the result is straightforward [23]. The $\alpha$-decay width to a final state with angular momentum $l$ is given by

$$\Gamma_l = \hbar v \left[\frac{R_\alpha}{G_l(R_\alpha)}\right]^2 [\mathcal{F}_l(R_\alpha)]^2 \equiv P_l F_l, \tag{2.21}$$

where $v$ is the c.m. velocity of the emitted $\alpha$ particle and $G_l(R_\alpha)$ is the irregular Coulomb wave function on some point beyond the nuclear surface. This quantity is a product of two functions strongly depending on the radius $R_\alpha$ but should be practically a constant in a region around the geometrical touching point between the $\alpha$ particle and the daughter nucleus. This is a very important test of the procedure which will be analyzed in the next section.

The four-particle creation operator in Eq. (2.9) is a superposition of the $pp-nn$ or $pn-pn$ quartets. The configuration counterpart of the pair-creation operators entering these quartets has the following form:

$$\begin{aligned}(c_{\tau_1 i}^\dagger c_{\tau_2 j}^\dagger)_{\alpha_2} &\rightarrow \mathcal{A}\{\psi_{\gamma_{\tau_1 i}}^{(\lambda_i)}(\xi_1)\psi_{\gamma_{\tau_2 j}}^{(\lambda_j)}(\xi_2)\}_{\alpha_2} \\ &\equiv \frac{1}{\sqrt{2}}\{[\psi_{\gamma_{\tau_1 i}}(\xi_1)\psi_{\gamma_{\tau_2 j}}(\xi_2)]_{\alpha_2} \\ &\quad - [\psi_{\gamma_{\tau_1 i}}(\xi_2)\psi_{\gamma_{\tau_2 j}}(\xi_1)]_{\alpha_2}\}. \end{aligned} \tag{2.22}$$

To estimate the overlap integral (2.20), when the above mentioned radial sp wave functions are given as numerical solutions of the Schrödinger equation, is a difficult task, due to change from absolute to the c.m. and relative coordinates. In Ref. [24] one introduces a method to estimate such an integral for the monopole ($l=0$) case and in Ref. [25] this technique is used to estimate the formation amplitude for the $\alpha$ decay of $^{212}$Po.

The main difficulty consists in the nonseparability between the radial and angular coordinates in the new system. It is therefore necessary to perform an angular integration before integrating over the radial coordinates. There is one case in which this operation can be done analytically, namely the spherical ho basis, by using Talmi-Moshinsky recoupling coefficients. As we shall show in the next section it is possible to have a very good representation of the sp wave functions $\psi_{\gamma_{\tau j}}(\xi)$ in terms of the ho basis, even for the real part of the narrow Gamow resonances

$$\psi_{\gamma_{\tau j}}(\xi) \equiv \sum_n c_n(\gamma_{\tau j})\varphi_{nljm}^{(\lambda)}(\xi), \quad \gamma_{\tau j} \equiv (\epsilon_\tau lj), \tag{2.23}$$

where the following standard definitions were used:

$$\varphi^{(\lambda)}_{nljm}(\xi)\equiv[\phi^{(\lambda)}_{nl}(\vec{r})\chi_{1/2}(s)]_{jm},$$
$$\phi^{(\lambda)}_{nlm}(\vec{r})\equiv\mathcal{R}^{(\lambda)}_{nl}(r)Y_{lm}(\hat{r}). \tag{2.24}$$

Here $\epsilon_\tau$ is the sp eigenvalue in the Woods-Saxon (WS) mean field for the $\tau=\pi,\nu$ particle, $c_n(\gamma_{\tau j})$ the expansion coefficients in the spherical ho basis and λ is the ho parameter. This parameter together with the expansion coefficients is determined by a fitting procedure of the sp state. We will consider together with the discrete negative-energy spectrum the narrow Gamow resonances with $\mathrm{Re}(E)>0$, $|\mathrm{Im}(E)|<1$ MeV.

Let us first consider in the structure of the quartet operator (2.8) the $pp-nn$ component. The pair $pp$ building block is given by the product of the sp wave functions entering the ho basis. By changing the $j-j$ to the $L-S$ coupling scheme only the singlet component gives contribution in the overlap with the $\alpha$-particle wave function. Then the configuration part can be be written in the relative+c.m. system using the Talmi-Moshinsky transformation. Finally, the overlap of the $pp$ part of the TDA wave function with the two-proton part of the $\alpha$-particle wave function (2.16) is given by the following expansion in terms of the ho wave functions:

$$\int d\xi_\pi[\phi^{(\lambda_\alpha)}_{00}(\vec{r}_\pi)\chi^{(\pi)}_{00}(12)]^*\sum_{1\leqslant 2}\frac{1}{\Delta_{12}}X_{\pi\pi}(\gamma_{\pi1}\gamma_{\pi2};\alpha_2a_2)\mathcal{A}\{\psi^{(\lambda)}_{\gamma_{\pi1}}(\xi_1)\psi^{(\lambda)}_{\gamma_{\pi2}}(\xi_2)\}_{\alpha_2}=\sum_{N_\pi}G_\pi(N_\pi;\alpha_2a_2)\Phi^{(\lambda)}_{N_\pi\alpha_2}(\vec{R}_\pi), \tag{2.25}$$

where we have introduced the $pp$ $G$ coefficients as

$$G_\pi(N_\pi;\alpha_2a_2)\equiv\sum_{12}B_\pi(n_1l_1j_1n_2l_2j_2;\alpha_2a_2)\left\langle(l_1l_2)\alpha_2\left(\frac{1}{2}\frac{1}{2}\right)0;\alpha_2\middle|\left(l_1\frac{1}{2}\right)j_1\left(l_2\frac{1}{2}\right)j_2;\alpha_2\right\rangle$$
$$\times\sum_{n_\pi}\langle n_\pi0N_\pi\alpha_2;\alpha_2|n_1l_1n_2l_2;\alpha_2\rangle\mathcal{I}^{(\lambda\lambda_\alpha)}_{n_\pi0}. \tag{2.26}$$

Here the first angular brackets denote the recoupling $jj-LS$ while the second ones denote the Talmi-Moshinsky coefficients, and

$$B_\pi(n_1l_1j_1n_2l_2j_2;\alpha_2a_2)\equiv\sqrt{2}\sum_{\epsilon_{\pi1}\leqslant\epsilon_{\pi2}}\frac{1}{\Delta_{12}}X_{\pi\pi}(\gamma_{\pi1}\gamma_{\pi2};\alpha_2a_2)c_{n_1}(\gamma_{\pi1})c_{n_2}(\gamma_{\pi2}). \tag{2.27}$$

The overlap integral between the spherical ho radial functions is defined as

$$\mathcal{I}^{(\lambda\lambda_\alpha)}_{n0}\equiv\langle\mathcal{R}^{(\lambda)}_{n0}|\mathcal{R}^{(\lambda_\alpha)}_{00}\rangle. \tag{2.28}$$

One also obtains similar $nn$ and $pn$ expansions.

By performing the transformation of the $pp-nn$ product to the relative+c.m. coordinates of the $\alpha$-particle, one finally obtains the overlap integral, defining the $pp-nn$ part of the formation amplitude. It is written as a superposition of the ho functions in the c.m. coordinate of the $\alpha$ cluster

$$\langle A|B\rangle\equiv\mathcal{F}_{\alpha_4a_4}(R_\alpha)Y_{\alpha_4}(\hat{R}_\alpha)=\sum_{N_\alpha}W_{\pi\nu}(N_\alpha;\alpha_4a_4)\Phi^{(\lambda)}_{N_\alpha\alpha_4}(\vec{R}_\alpha), \tag{2.29}$$

where

$$W_{\pi\nu}(N_\alpha;\alpha_4a_4)\equiv8\sum_{N_\pi N_\nu}\sum_{\alpha_2a_2\beta_2b_2}G_\pi(N_\pi;\alpha_2a_2)G_\nu(N_\nu;\beta_2b_2)$$
$$\times X(pp\alpha_2a_2;nn\beta_2b_2;\alpha_4a_4)\sum_{n_\alpha}\langle n_\alpha0N_\alpha\alpha_4;\alpha_4|N_\pi\alpha_2N_\nu\beta_2;\alpha_4\rangle\mathcal{I}^{(\lambda\lambda_\alpha)}_{n_\alpha0}. \tag{2.30}$$

The second part of the overlap integral is given by the $pn-pn$ four-particle component. It is computed in a similar way, by replacing the four-particle amplitude and $G$ coefficients with the corresponding $pn$ terms. To do this one uses the equivalent $pn$ representation of the $\alpha$-particle wave function (2.16), by exchanging the ''2'' and ''3'' coordinates:

TABLE I. Single-particle energies used in the two-particle basis (in MeV) for protons (a) and neutrons (b).

(a)

| $k$ | $l$ | $2j$ | Re($\epsilon_k$) | Im($\epsilon_k$) |
|---|---|---|---|---|
| 1 | 5 | 9 | −3.571 | 0.000 |
| 2 | 3 | 7 | −3.333 | 0.000 |
| 3 | 6 | 13 | −1.605 | 0.000 |
| 4 | 1 | 3 | −0.485 | 0.000 |
| 5 | 3 | 5 | −0.306 | 0.000 |
| 6 | 1 | 1 | 0.696 | 0.000 |
| 7 | 4 | 9 | 4.264 | 0.000 |
| 8 | 6 | 11 | 5.689 | 0.000 |
| 9 | 7 | 15 | 6.240 | 0.000 |
| 10 | 2 | 5 | 6.954 | −0.003 |
| 11 | 0 | 1 | 8.017 | −0.047 |
| 12 | 4 | 7 | 8.316 | −0.001 |
| 13 | 2 | 3 | 8.717 | −0.036 |
| 14 | 5 | 11 | 11.633 | −0.027 |

(b)

| $k$ | $l$ | $2j$ | Re($\epsilon_k$) | Im($\epsilon_k$) |
|---|---|---|---|---|
| 1 | 4 | 9 | −3.690 | 0.000 |
| 2 | 6 | 11 | −2.538 | 0.000 |
| 3 | 2 | 5 | −1.876 | 0.000 |
| 4 | 7 | 15 | −1.601 | 0.000 |
| 5 | 0 | 1 | −1.283 | 0.000 |
| 6 | 2 | 3 | −0.614 | 0.000 |
| 7 | 4 | 7 | −0.546 | 0.000 |
| 8 | 3 | 7 | 2.199 | −0.998 |
| 9 | 5 | 11 | 2.472 | −0.038 |
| 10 | 8 | 17 | 5.348 | −0.002 |
| 11 | 5 | 9 | 5.594 | −0.808 |
| 12 | 7 | 13 | 5.701 | −0.013 |
| 13 | 9 | 19 | 12.368 | −0.108 |

$$\psi_\alpha(\xi_\alpha) \equiv \phi_{00}^{(\lambda_\alpha)}(\vec{r}_{12})\,\phi_{00}^{(\lambda_\alpha)}(\vec{r}_{34})\,\phi_{00}^{(\lambda_\alpha)}(\vec{r}_{12-34}) \times \chi_{00}^{(\pi)}(12)\,\chi_{00}^{(\nu)}(34) = \phi_{00}^{(\lambda_\alpha)}(\vec{r}_{13})\,\phi_{00}^{(\lambda_\alpha)}(\vec{r}_{24})\,\phi_{00}^{(\lambda_\alpha)}(\vec{r}_{13-24}) \times \chi_{00}^{(\pi\nu)}(13)\,\chi_{00}^{(\pi\nu)}(24). \tag{2.31}$$

## III. NUMERICAL APPLICATION

### A. Single-particle basis

The sp spectrum is provided by the numerical integration of the radial Schrödinger equation. We used as a mean field the Woods-Saxon (WS) potential with the so called universal parametrization [26]. The bound states and resonances in continuum were computed using the code ''Gamow'' [27] in a revised version. The results for $^{208}$Pb are given in Tables I(a) and I(b) for protons and neutrons, respectively. Here the states are labeled by the index $k$. The angular momentum $l$ and total spin $j$ are also given. Concerning the resonances in continuum only those states having energies with Re($\epsilon_k$) $<12.5$ MeV and $|\mathrm{Im}(\epsilon_k)|<1$ MeV were selected. One can see that there are more narrow proton resonances due to the Coulomb barrier. The calculated values are rather close to those obtained in Ref. [12] were a different parametrization of the WS potential was used. In principle, the continuum part of the spectrum, which we have neglected, contains the background given by the integration on a contour around the included resonances.

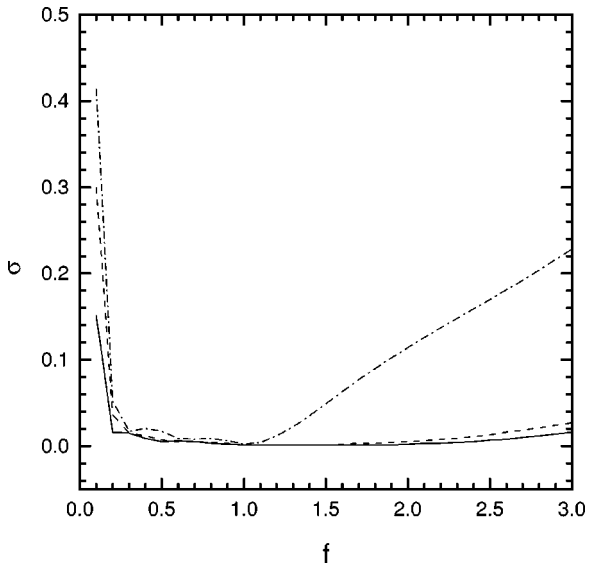


FIG. 1. The error $\sigma$ defined by Eq. (3.2) versus the parameter $f$ defined by Eq. (3.1).

In order to perform the overlap integral (2.15) it is necessary to expand the sp wave functions in terms of the spherical ho basis as in Eq. (2.23). The expansion coefficients are found by a standard fitting procedure for a given ho parameter $\lambda$. Let us define the parameter $f$ as the coefficient multiplying the standard ho parameter

$$\lambda = f\lambda_0, \quad \lambda_0 = \frac{M_N\omega}{\hbar}. \tag{3.1}$$

In Fig. 1 we plot, as a function of $f$, the error $\sigma$ in replacing the numerical solution of the radial Schrödinger equation by an expansion in terms of the ho basis. This error is defined by the following relation:

$$\sigma \equiv \left[ \int_{R_{\min}}^{R_{\max}} \left| \mathrm{Re}[\psi_k(R)] - \sum_{n=0}^{n_{\max}} c_{kn} \mathcal{R}_{nl}^{(\lambda)}(R) \right|^2 R^2 dR \right]^{1/2}. \tag{3.2}$$

We have chosen some high-spin proton states as typical examples: a bound state labeled by $k=3$ in Table I(a) (solid line) and two Gamow resonances with $k=9$ (dashed line) and $k=14$ (dot-dashed line). In Eq. (3.2) the limits of integration are $R_{\min}=0$ fm, $R_{\max}=15$ fm. The maximal value of the radial quantum number is taken as $n_{\max}=9$ for which saturation is always obtained. One can observe that for a rather large interval of the coefficient $f$ the approximation is very good, even for the real part of the Gamow wave func-

TABLE II. Experimental and theoretical excitation energies in $^{210}$Po (a), $^{210}$Pb (b), and $^{210}$Bi (c). All experimentally known states are taken below 2.5 MeV for $^{210}$Po, below 2.0 MeV for $^{210}$Pb, and below 1.0 MeV for $^{210}$Bi. Also the experimental and theoretical BE$(2;J_i \to J_f)$ values are given in Weisskopf units in panel (d). The bare proton charge ($e^{(p)}=1.0e$) and the effective neutron charge $e^{(n)}_{\rm eff}=1.1e$ were used in the calculation. The experimental data were taken from [31,32].

(a)

| $J^\pi_{a_2}$ | $E_{\rm expt}$ [MeV] | $E_{\rm theor}$ [MeV] |
|---|---|---|
| $0^+_1$ | 0.000 | 0.000 |
| $2^+_1$ | 1.181 | 1.280 |
| $4^+_1$ | 1.427 | 1.447 |
| $6^+_1$ | 1.473 | 1.483 |
| $8^+_1$ | 1.557 | 1.493 |
| $8^+_2$ | 2.188 | 1.618 |
| $2^+_2$ | 2.290 | 1.650 |
| $6^+_2$ | 2.326 | 1.669 |
| $4^+_2$ | 2.383 | 1.675 |
| $3^-_1$ | 2.387 | |
| $1^+_1$ | 2.394 | 1.746 |
| $5^+_1$ | 2.403 | 1.746 |
| $3^+_1$ | 2.414 | 1.746 |
| $7^+_1$ | 2.438 | 1.746 |

(c)

| $J^\pi_{a_2}$ | $E_{\rm expt}$ [MeV] | $E_{\rm theor}$ [MeV] |
|---|---|---|
| $1^-_1$ | 0.000 | 0.000 |
| $0^-_1$ | 0.047 | 0.338 |
| $9^-_1$ | 0.271 | 0.262 |
| $2^-_1$ | 0.320 | 0.338 |
| $3^-_1$ | 0.348 | 0.235 |
| $7^-_1$ | 0.433 | 0.284 |
| $5^-_1$ | 0.439 | 0.274 |
| $4^-_1$ | 0.502 | 0.338 |
| $6^-_1$ | 0.550 | 0.338 |
| $(1^-_2)$ | 0.563 | 0.310 |
| $8^-_1$ | 0.583 | 0.338 |
| $10^-_1$ | 0.670 | 1.431 |
| $8^-_2$ | 0.916 | 0.416 |
| $(2^-_2)$ | 0.972 | 0.422 |

(b) (d)

| $J^\pi_{a_2}$ | $E_{\rm expt}$ [MeV] | $E_{\rm theor}$ [MeV] | $J_i$ | $J_f$ | Expt.($^{210}$Pb) | Theor.($^{210}$Pb) | Expt.($^{210}$Po) | Theor.($^{210}$Po) |
|---|---|---|---|---|---|---|---|---|
| $0^+_1$ | 0.000 | 0.000 | 2 | 0 | 1.4(4) | 1.38 | 0.56(12) | 0.62 |
| $2^+_1$ | 0.800 | 0.903 | 4 | 2 | 4.8(9) | 2.23 | 4.53(15) | 1.23 |
| $4^+_1$ | 1.098 | 1.027 | 6 | 4 | 2.1(8) | 1.64 | 3.00(12) | 1.17 |
| $6^+_1$ | 1.196 | 1.076 | 8 | 6 | 0.7(3) | 0.65 | 1.10(5) | 0.48 |
| $8^+_1$ | 1.279 | 1.103 | | | | | | |
| $(10^+_1)$ | 1.799 | 2.101 | | | | | | |
| $3^-_1$ | 1.870 | | | | | | | |
| $(8^+_2)$ | 2.003 | 2.191 | | | | | | |
| $(4^+_2)$ | 2.038 | 2.223 | | | | | | |

tion (the imaginary part is negligible for narrow resonances). The minimum of $\sigma$ is reached around $f=1$ for all considered states in Tables I(a) and I(b) and we have chosen in our calculations this value, corresponding to the standard ho parameter. We have checked the expansion (2.23) by the direct diagonalization of the WS mean field in the ho basis. The coefficients of the bound states are very close to those obtained by the above fitting procedure. Concerning the states with positive energy the narrow resonances are embedded in the quasicontinuum background. They can be selected using a standard phase-shift analysis.

### B. Two-particle states

The two-particle states were treated by using Eq. (2.6) with the two-body interaction matrix elements obtained from the surface delta force [28] with one adjustable strength-scaling parameter for each of the neutron-neutron, proton-proton, and proton-neutron interaction channels. These three parameters were adjusted in the nuclei $^{210}$Pb, $^{210}$Po, and $^{210}$Bi, respectively, to yield reasonable values for the energies of the lowest states in these nuclei. In addition, the values of the radial single-particle functions on the nuclear surface were evaluated for the surface delta force and not approximated by one single constant as discussed in [28].

In Tables II(a)–II(c) we list the available experimental data for the nuclei $^{210}$Po, $^{210}$Pb, and $^{210}$Bi, respectively. Also the corresponding calculated values are given for comparison. One notices that for all of these nuclei the lowest states of a given multipolarity $\alpha^\pi_2=J^\pi$ are very well reproduced by the surface delta interaction (for all the multipoles we have used the one and the same interaction-strength parameter mentioned above). For $^{210}$Po and $^{210}$Bi the second calculated state of a given multipole falls well below the experimental second state producing a too compressed spectrum around 1.5 MeV in $^{210}$Po and around 0.5 MeV in $^{210}$Bi. In $^{210}$Pb and $^{210}$Po the first $3^-$ state is very collective [can be seen from the reduced octupole transition strength $B(E3)$ which exceeds 20 Weisskopf units for both nuclei] and most likely of the three-particle–one-hole character which is outside our configuration space. This is why no counterpart of it is given on the theoretical side in Tables II(a) and II(b). From Table II(d) one can see that the known $B(E2)$ values of $^{210}$Pb

TABLE III. Low-lying excitation energies in $^{212}$Po (in MeV) for different thresholds of the metric matrix eigenvalues (in parentheses). The experimental data are taken from [31].

| $J^{\pi}_{a_4}$ | $E_{\rm expt}$ | $E(0.05)$ | $E(0.2)$ | $E(0.5)$ |
|---|---|---|---|---|
| $0^+_1$ | 0.000 | 0.000 | 0.000 | 0.000 |
| $2^+_1$ | 0.727 | 0.949 | 0.952 | 0.952 |
| $4^+_1$ | 1.132 | 1.087 | 1.090 | 1.081 |
| $6^+_1$ | 1.355 | 1.081 | 1.144 | 1.135 |
| $8^+_1$ | 1.476 | 1.131 | 1.174 | 1.166 |
| $2^+_2$ | 1.513 | 1.203 | 1.203 | 2.398 |
| $1^+_1$ | 1.621 | 1.907 | 1.909 | 1.901 |
| $2^+_3$ | 1.679 | 1.783 | 1.995 | 2.423 |
| $0^+_2$ | 1.801 | 2.080 | 2.091 | 2.081 |
| $2^+_4$ | 1.806 | 2.248 | 2.253 | 2.607 |

and $^{210}$Po are reasonably well reproduced by the theory for the bare value of the proton charge ($e^{(p)}=1.0e$) and the effective neutron charge $e^{(n)}_{\rm eff}=1.1e$.

### C. $\alpha$-like states

First of all, in order to have confidence in the description of the high-lying four-particle resonances, the known low-lying states in $^{212}$Po should be reproduced. They were computed in Refs. [19] using a method similar to the MSM approach and in Ref. [29] within the shell model approach. In the latter paper a very good agreement was obtained for the first $0^+,2^+,4^+,6^+,8^+$ states. As mentioned earlier, our initial MSM basis in nonorthogonal and overcomplete, and a new orthogonal basis obtained using the eigenstates of the metric matrix (B5) should be used. The states having small metric eigenvalues are spurious and should be excluded. This is due to the fact that $pn-pn$ four-particle basis can be expressed in terms of the $pp-nn$ basis if all the two-particle eigenstates are used. In our calculation we used only the lowest two-particle $pp,nn,pn$ eigenstates for multipoles up to $\alpha_4=J=9$ and only some components become spurious. The result of calculation is given in Table III where in the second column are given the experimental energies and in the next three columns the computed eigenvalues by solving Eq. (2.11). They correspond to different minimal accepted eigenvalues $D_{\rm min}$ of the metric matrix, written in parantheses. One can observe that the energies in the third and fourth columns, corresponding to $D_{\rm min}=0.05$ and $D_{\rm min}=0.2$, respectivelly, are practically identical and they reproduce the experimental data within 400 keV. The values of the last column, corresponding to $D_{\rm min}=0.5$, are worse and therefore we fixed the minimal threshold of the metric matrix eigenvalues at $D_{\rm min}=0.2$. One can see that, in spite of the fact that only the lowest two-particle states were included in calculation, the ageement with the experimental low-lying part of the spectrum is quite satisfactory, somewhere between Ref. [19] and Ref. [29].

It is now important to analyze the structure of these four-particle states in tems of the two-particle states, containing Gamow sp resonances. In Table IV (second column) is given the structure of the four-particle states in terms of the most important two-particle pairs. One can see that the first six low-lying states have practically one major component. The four-particle amplitude $X$, computed according to Eq. (B8), is given in the third column and it is larger than unity, due to the nonorthogonality of the basis. It is important to stress the fact that the lowest monopole two-particle components $0^+_1(pp)$ and $0^+_1(nn)$, entering in the four-particle wave function, are the only ones having in their structure Gamow resonances in continuum. This can be seen in Tables V(a) and VI(a) where we give the structure of these states in terms of the sp states labeled in Tables I(a) and I(b) for protons and neutrons, respectively. The other low-lying states in Table III, which are not given in Table IV, have no such states in their structure. It is important to mention that the g.s. structure of $^{212}$Po is practically of the form g.s.($^{210}$Po) $\otimes$ gs($^{210}$Pb) in agreement with the supposed ansatz of Refs. [21,22].

TABLE IV. Quartet structure of the low-lying $\alpha$-like states in terms of the two-particle pairs (the second column). The amplitude is given in the third column. Given are also the spectroscopic factors of the $pp-nn$ (the fourth column) and $pn-pn$ (the fifth column) four-particle terms in the quartet operator defined by Eq. (2.9). In the sixth and seventh columns are given the hindrance factors of the $J^{\pi}_{a_4}$ states defined by Eq. (3.6).

| $J^{\pi}_{a_4}$ | $J(pp),J(nn)$ | $X$ | $S_1$ | $S_2$ | HF$_1$ | HF$_2$ |
|---|---|---|---|---|---|---|
| $0^+_1$ | $0^+_1(pp),0^+_1(nn)$ | 1.084 | 1.19(−2) | 8.49(−7) | 1.00 | 1.00 |
| $2^+_1$ | $0^+_1(pp),2^+_1(nn)$ | 1.091 | 1.38(−3) | 5.16(−8) | 0.12 | 0.06 |
| $4^+_1$ | $0^+_1(pp),4^+_1(nn)$ | 1.092 | 7.49(−4) | 1.39(−9) | 0.07 | 0.00 |
| $6^+_1$ | $0^+_1(pp),6^+_1(nn)$ | 1.092 | 4.44(−4) | 1.02(−8) | 0.04 | 0.01 |
| $8^+_1$ | $0^+_1(pp),8^+_1(nn)$ | 1.092 | 3.33(−4) | 5.36(−9) | 0.02 | 0.00 |
| $2^+_2$ | $2^+_1(pp),0^+_1(nn)$ | 1.092 | 1.54(−3) | 6.44(−8) | 0.04 | 0.73 |

This microscopic structure of the four-particle states is strongly connected with the formation amplitude (2.29) computed as the overlap integral between these states and the $\alpha$-particle wave function. It is a function of the distance between the daughter and the c.m. of the emitted cluster. The most impotant $\alpha$ decay of $^{212}$Po is the transition from the g.s. $0^+_1$. In Fig. 2 we plot the formation ampitude for this transition versus the mentioned distance. One can observe that this function is peaked on the nuclear surface $R_0=1.2A^{1/3}=7.2$ fm. It is of interest to see which would be the equivalent local potential if one considers the $\alpha$-particle formation amplitude as a wave function satisfying the Schrödinger equation

$$-\frac{\hbar^2}{2M_\alpha}\nabla^2\mathcal{F}_l(R)+V_l(R)\mathcal{F}_l(R)=E_\alpha\mathcal{F}_l(R), \qquad (3.3)$$

where we have denoted the $\alpha$-particle c.m. radius by $R\equiv R_\alpha/2$, the angular momentum by $\alpha_4=l$ and dropped the eigenvalue index.

By taking into account the expansion (2.29) one obtains for the unknown potential the relation

TABLE V. The structure of the two-particle states $0^+_{a_2}(pp)$ in $^{210}$Po containing proton single-particle Gamow resonances. The amplitude is given in the second column. In the third and fourth columns are given the involved single-particle states labeled according to the first column of Table I(a).

| | (a) $0^+_1(pp)E=-8.651$ MeV | | | (b) $0^+_4(pp)E=-1.547$ MeV | | | (c) $0^+_6(pp)E=1.219$ MeV | | |
|---|---|---|---|---|---|---|---|---|---|
| No. | $X$ | $k_1(p)$ | $k_2(p)$ | $X$ | $k_1(p)$ | $k_2(p)$ | $X$ | $k_1(p)$ | $k_2(p)$ |
| 1 | 0.460 | 1 | 1 | −0.111 | 2 | 2 | 0.111 | 4 | 4 |
| 2 | 0.771 | 2 | 2 | 0.379 | 3 | 3 | 0.132 | 5 | 5 |
| 3 | −0.313 | 3 | 3 | 0.769 | 4 | 4 | −0.977 | 6 | 6 |
| 4 | 0.156 | 4 | 4 | 0.475 | 5 | 5 | | | |
| 5 | 0.149 | 5 | 5 | 0.106 | 6 | 6 | | | |
| 6 | −0.124 | 7 | 7 | | | | | | |
| 7 | 0.115 | 9 | 9 | | | | | | |

| | (d) $0^+_7(pp)E=6.598$ MeV | | | (e) $0^+_8(pp)E=10.617$ MeV | | |
|---|---|---|---|---|---|---|
| No. | $X$ | $k_1(p)$ | $k_2(p)$ | $X$ | $k_1(p)$ | $k_2(p)$ |
| 1 | 0.135 | 3 | 3 | 0.443 | 7 | 7 |
| 2 | −0.123 | 4 | 4 | −0.647 | 8 | 8 |
| 3 | −0.129 | 5 | 5 | 0.563 | 9 | 9 |
| 4 | −0.125 | 6 | 6 | −0.182 | 10 | 10 |
| 5 | −0.859 | 7 | 7 | −0.130 | 12 | 12 |
| 6 | −0.185 | 8 | 8 | | | |
| 7 | 0.320 | 9 | 9 | | | |
| 8 | −0.146 | 10 | 10 | | | |
| 9 | −0.139 | 12 | 12 | | | |

$$V_l(R)=E_\alpha+\hbar\omega\frac{4\lambda}{\lambda_\alpha\mathcal{F}_l(R)}\sum_{N_\alpha}W_{\pi\nu}(N_\alpha;l1)\times\left[2\lambda R^2-2N_\alpha-l-\frac{3}{2}\right]\mathcal{R}^{(4\lambda)}_{N_\alpha l}(R). \quad (3.4)$$

In Fig. 3 we depict this equivalent potential for $l=0$ (solid curve) corresponding to the formation amplitude in Fig. 2. One clearly sees the molecular shape of this local equivalent potential. This kind of local potential was used in some previous works as a phenomenological interaction to reproduce

TABLE VI. The structure of the two-particle states $0^+_{a_2}(nn)$ in $^{210}$Pb containing neutron single-particle Gamow resonances. The amplitude is given in the second column. In the third and fourth columns are given the single-particle states labeled according to the first column of Table I(b).

| | (a) $0^+_1(nn)E=-8.510$ MeV | | | (b) $0^+_6(nn)E=-1.424$ MeV | | |
|---|---|---|---|---|---|---|
| No. | $X$ | $k_1(n)$ | $k_2(n)$ | $X$ | $k_1(n)$ | $k_2(n)$ |
| 1 | −0.896 | 1 | 1 | −0.137 | 3 | 3 |
| 2 | −0.305 | 2 | 2 | 0.926 | 6 | 6 |
| 3 | −0.240 | 3 | 3 | 0.321 | 7 | 7 |
| 4 | 0.106 | 4 | 4 | | | |
| 5 | −0.110 | 10 | 10 | | | |

| | (c) $0^+_7(nn)E=-1.115$ MeV | | | (d) $0^+_8(nn)=4.398$ MeV | | |
|---|---|---|---|---|---|---|
| No. | $X$ | $k_1(n)$ | $k_2(n)$ | $X$ | $k_1(n)$ | $k_2(n)$ |
| 1 | −0.335 | 6 | 6 | −1.000 | 8 | 8 |
| 2 | 0.941 | 7 | 7 | | | |

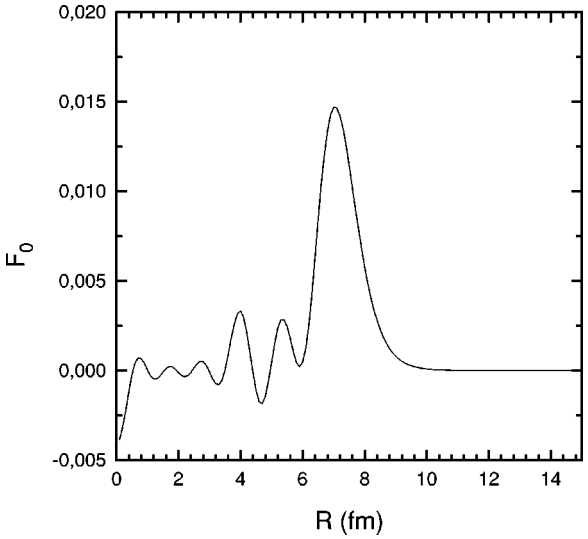


FIG. 2. The $\alpha$-particle formation amplitude given by Eq. (2.29) for the ground-state-to-ground-state transition versus the distance $R$ of the center of mass of the $\alpha$ particle from the daughter nucleus $^{208}$Pb.

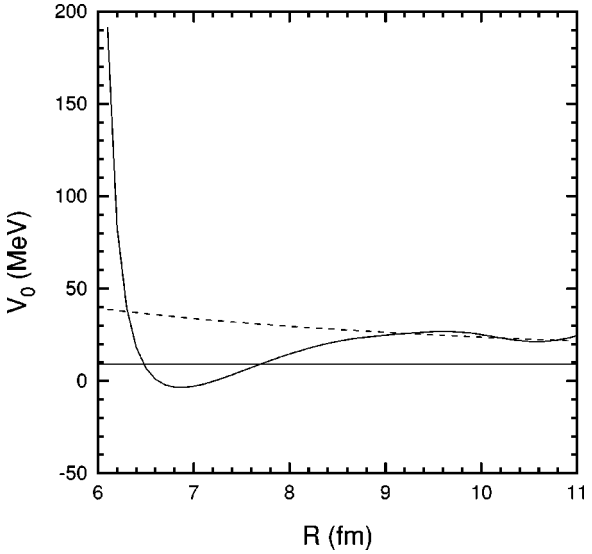


FIG. 3. The local equivalent potential computed using Eq. (3.4) corresponding to the $\alpha$-particle wave function in Fig. 2. By a dashed line it is plotted the $\alpha$-daughter Coulomb potential. Horizontal solid line shows the energy of the emitted $\alpha$ particle.

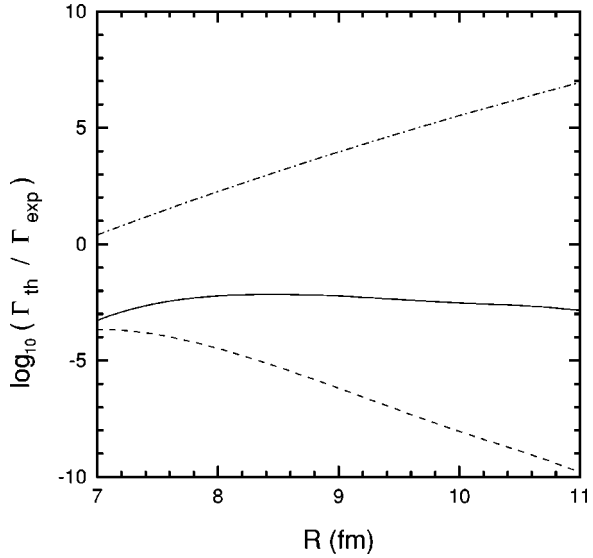


FIG. 4. The quantities $\log(\Gamma_{th}/\Gamma_{exp})$ (solid line), $\log(F_0)$ (dashed line), and $\log(P_0/\Gamma_{exp})$ (dot-dashed line) as functions of the distance $R$ of the center of mass of the $\alpha$ particle from the daughter nucleus $^{208}$Pb. $F_0$ and $P_0$ are defined by Eq. (2.21).

quasimolecular resonances in the $\alpha$-particle scattering data [17]. By a dashed line we indicate the pure Coulomb potential between the daughter and $\alpha$-particle. After the geometrical touching radius $R_c \equiv 1.2(A_A^{1/3}+A_\alpha^{1/3})=9$ fm the equivalent potential bears a close resemblance to the Coulomb interaction. The Coulomb barrier at this point is around 25 MeV. The solid horizontal line denotes the energy of the emitted $\alpha$-particle $E_\alpha=8.95$ MeV, which actually is the gs energy of the $^{212}$Po nucleus with respect to $^{208}$Pb. All the excitation energies in Table III are given relative to this energy.

The following integral of the formation probability defines the so called spectroscopic factor (SF):

$$S_{ila_4} \equiv \int_0^\infty |\mathcal{F}_{ila_4}(R)|^2 R^2 dR, \tag{3.5}$$

where $i=1$ corresponds to the $pp-nn$ component and $i=2$ to the $pn-pn$ component in the four-particle wave function (2.8). In the fourth and fifth columns of Table IV are given the spectroscopic factors for the $pp-nn$ and $pn-pn$ four-particle components of the wave function. One can observe, first of all, that the total g.s. to g.s. SF has the right order of magnitude [30] and is practically given by the $pp-nn$ component which is much larger that the $pn-pn$ one. This means that the $pn$ overlap is much smaller in comparison with the $pp$ and $nn$ overlaps because proton and neutron shells above $^{208}$Pb are different. The other states have smaller SF. In the sixth and seventh columns there are given the so called hindrance factors $\mathrm{HF}_i$ defined as a mean value on the interval [8,10] fm of the ratio

$$\mathrm{HF}_{ila_4} \equiv \overline{\left|\frac{\mathcal{F}_{ila_4}(R)}{\mathcal{F}_{i01}(R)}\right|^2}. \tag{3.6}$$

The states given in Table IV have $\mathrm{HF}_1>0.01$. The other states in Table III, not given in Table IV, have much smaller HF and have no sp Gamow resonances in their structure. Therefore, there is a straightforward connection between the sp Gamow states and the magnitude of the $\alpha$-particle overlap integral.

In spite of the strong decrease of the formation amplitude in the region of the geometrical touching radius $R_c$ the decay width, as can be seen from Fig. 4 (solid line), is practically constant, proving the validity of our calculation. This is the reason why we used the interval [8,10] fm to estimate the HF. According to Eq. (2.21) the decay width is a product of two terms which have an opposite behavior: the formation probability $F_0$ (dashed line in Fig. 4) is decreasing and the penetrability $P_0$ (dot-dashed line in Fig. 4) is increasing. It is important to observe from the same figure that the decay width is underestimated by two orders of magnitude. This means that the inclusion of narrow Gamow resonances is not enough in order to reproduce the absolute value of the decay width. The role of the ''background,'' given by the integration in the complex plane on a countour including the considered resonances, is also very important because the formation probability of an $\alpha$ cluster on the nucler surface is proportional to the density of the sp components in the continuum.

But, as it was pointed out, the narrow sp Gamow resonances play an important role in some low-lying states having a strong overlap with the $\alpha$-particle wave function and which are called $\alpha$-like states. They should also play an important role in some high-lying states seen as resonances in the scattering of $\alpha$ particles on the daughter nucleus, especially above the Coulomb barrier. The states above the bar-

TABLE VII. High-lying monopole ($0^+_{a_4}$) states with a large hindrance factor for the $pp-nn$ channel ($HF_1$, last column). The eigenvalue number is given in the first and energy in the second column. Their structure in terms of the two-particle proton states of Table V and neutron states of Table VI is given in the third column. In the fourth column there is given the spectroscopic factor of the $pp-nn$ quartet operator (2.9).

| $a_4$ | $E$ [MeV] | $J(pp),J(nn)$ | $X$ | $S_1$ | $HF_1$ |
|---|---|---|---|---|---|
| 141 | 6.332 | $0^+_4(pp),0^+_1(nn)$ | −0.667 | 1.34(−03) | 14.33 |
| | | $0^+_3(pp),0^+_2(nn)$ | 0.242 | | |
| | | $0^+_1(pp),0^+_6(nn)$ | 0.614 | | |
| 316 | 12.181 | $0^+_1(pp),0^+_8(nn)$ | 1.063 | 1.34(−03) | 14.33 |
| | | $0^+_2(pp),0^+_8(nn)$ | −0.366 | | |
| 356 | 14.494 | $0^+_7(pp),0^+_1(nn)$ | 1.036 | 2.66(−03) | 1.48 |
| 383 | 16.541 | $0^+_3(pp),0^+_8(nn)$ | −1.030 | 1.43(−04) | 2.93 |
| | | $0^+_2(pp),0^+_8(nn)$ | −0.136 | | |
| 438 | 19.338 | $0^+_4(pp),0^+_8(nn)$ | 1.002 | 6.88(−04) | 7.89 |
| 458 | 20.396 | $0^+_7(pp),0^+_5(nn)$ | −0.987 | 6.44(−04) | 1.70 |
| 472 | 21.662 | $0^+_7(pp),0^+_6(nn)$ | 1.001 | 1.02(−03) | 1.09 |
| 475 | 21.979 | $0^+_7(pp),0^+_7(nn)$ | 1.002 | 2.84(−04) | 1.28 |
| 476 | 22.100 | $0^+_6(pp),0^+_8(nn)$ | 1.000 | 2.05(−04) | 2.70 |
| 507 | 27.486 | $0^+_7(pp),0^+_8(nn)$ | 1.001 | 7.09(−04) | 21.98 |
| 510 | 31.499 | $0^+_8(pp),0^+_8(nn)$ | 1.000 | 8.97(−05) | 4.28 |

rier have energies larger than $16(=25-9)$ MeV. In Tables V and VI we list the structure of the two-particle states entering the four-particle eigenstates and containing sp Gamow states for protons and neutrons, respectively. The excitation energies are relative to the gs energy in $^{212}$Po. One can see that all of them have a monopole character.

In Table VII are given the monopole $\alpha$-like four-particle states having $HF_1>1$ (last column). To obtain such high lying states we performed a diagonalization using a much larger basis by considering the two-particle states with energies less than 20 MeV and $J=0,\ldots,4$. In spite of the very large amount of eigenstates only very few have large overlaps with the $\alpha$-particle wave function, i.e., large values of $HF_1$ and spectroscopic factors. All these states contain at least one of the states of Tables V or VI, containing Gamow resonances in their structure, as can be seen from the third column of Table VII. The high-lying $\alpha$-like quadrupole states are given in Table VIII. As in the previous case these states have two-particle monopole components carrying Gamow resonances and only two of them are above the Coulomb barrier.

## IV. CONCLUSIONS

In this article we have performed an analysis of the $\alpha$-like structure for low-lying and high-lying states in $^{212}$Po. We have chosen this nucleus as a very good example of a two-proton–two-neutron structure. The single-particle states were found as eigenstates in the Woods-Saxon mean field with the universal parametrization. Together with the particle bound states the narrow Gamow resonances in continuum were considered. We have used a modified (symmetric) version of the multistep shell model which describes, in the first step, two-particle $pp$, $nn$ and $pn$ states in $^{210}$Po, Pb, Bi nuclei, respectively. As a residual two-body potential we have used the surface delta interaction. It is very satisfactory that the low-lying states in $^{212}$Po can be reproduced using only the lowest two-particle eigenstates of these three nuclei as building blocks. In order to account for the Pauli principle, the spurious components with small eigenvalues of the metric matrix were excluded.

TABLE VIII. The same as in Table VII, but for the quadrupole ($2^+_{a_4}$) states.

| $a_4$ | $E$ [MeV] | $J(pp),J(nn)$ | $X$ | $S_1$ | $HF_1$ |
|---|---|---|---|---|---|
| 171 | 4.334 | $2^+_{11}(pp),0^+_8(nn)$ | 1.033 | 0.54(−04) | 1.48 |
| | | $2^+_{11}(pp),2^+_{19}(nn)$ | −0.114 | | |
| 409 | 11.034 | $0^+_7(pp),2^+_{19}(nn)$ | 1.009 | 0.18(−03) | 5.08 |
| 432 | 12.020 | $2^+_{16}(pp),0^+_8(nn)$ | 0.812 | 0.18(−03) | 5.08 |
| | | $2^+_{16}(pp),2^+_{19}(nn)$ | 0.589 | | |
| 485 | 18.087 | $0^+_{11}(pp),2^+_{19}(nn)$ | 1.000 | 0.35(−03) | 13.32 |
| 487 | 18.585 | $0^+_{11}(pp),2^+_{21}(nn)$ | 1.000 | 0.20(−03) | 1.28 |

We also propose an efficient technique to estimate the $\alpha$-particle formation amplitude by expanding the bound as well as the Gamow resonant states in terms of the ho basis with a standard ho parameter. By using this technique we have analyzed the $\alpha$-cluster content of the wave function for all four-particle eigenstates. We found that the first lowest states have an $\alpha$-particle formation amplitude comparable with that of the ground state and called them $\alpha$-like states. We also have found some high-lying monopole and quadrupole eigenstates strongly overlapping with the $\alpha$-cluster wave function. All of them have in their structure monopole two-particle states of $pp$ or $nn$ type, with important Gamow resonance components. The states above the Coulomb barrier should be observed as resonances in the $\alpha$-particle scattering on $^{208}$Pb. Moreover, the equivalent local potential, derived by evaluating the $\alpha$-particle formation amplitude for the transition between the ground states and interpreting it as a wave function satisfying the Schrödinger equation, has a ''pocket'' molecular shape. Similar potentials were used in calculations reproducing such resonances in the elastic scattering of $\alpha$-particles. Most of such resonances were observed in light nuclei around Ca and therefore our future purpose is to extend the multistep shell-model calculation into this region.

It turned out that the spectroscopic factor of the $pp-nn$ component is much larger than that of the $pn-pn$ component owing to the difference in the proton and neutron single-particle structures. In addition, the $pp-nn$ component has the right order of magnitude. The absolute value of the ground-state-to-ground-state decay width is underestimated by two orders of magnitude, but this can be understood by noticing that the backgrond part of the continuum single-particle spectrum was completely omitted. This does not affect the relative hindrance factors and the shape of the equivalent local $\alpha$-cluster–daughter potential. The inclusion of the background components into the computation will be presented in a forthcoming paper.

**ACKNOWLEDGMENTS**

One of us (D.S.D.) is grateful for the financial support given by Finnish Academy during his stay in Jyväskylä, where part of this work was performed. Discussions with R.J. Liotta (Stockholm), T. Vertse (Debrecen), P.O. Lipas (Jyväskylä), T. Lönnroth (Turku), and A. Sǎndulescu (Bucharest) are gratefully acknowledged.

## APPENDIX A: FOUR-PARTICLE METRIC MATRIX

The metric matrix is given by the following relations:

$$\langle 0|(P_{\beta_2}(nn;b_2)P_{\alpha_2}(pp;a_2))_{\alpha_4}(P^{\dagger}_{\alpha_2'}(pp;a_2')P^{\dagger}_{\beta_2'}(nn;b_2'))_{\alpha_4}|0\rangle=\delta_{\alpha_2\alpha_2'}\delta_{\beta_2\beta_2'}\delta_{a_2a_2'}\delta_{b_2b_2'}, \tag{A1}$$

$$\begin{aligned}\langle 0|(P_{\beta_2}(np;b_2)P_{\alpha_2}(np;a_2))_{\alpha_4}(P^{\dagger}_{\alpha_2'}(pn;a_2')P^{\dagger}_{\beta_2'}(pn;b_2'))_{\alpha_4}|0\rangle&=\delta_{\alpha_2\alpha_2'}\delta_{\beta_2\beta_2'}\delta_{a_2a_2'}\delta_{b_2b_2'}+\delta_{\alpha_2\beta_2'}\delta_{\beta_2\alpha_2'}\delta_{a_2b_2'}\delta_{b_2a_2'}(-)^{\alpha_2+\beta_2-\alpha_4}\\&-\sum_{ijkl}[A(ijkl;\alpha_2a_2\beta_2b_2\alpha_2'a_2'\beta_2'b_2')\\&+A(ijkl;\alpha_2a_2\beta_2b_2\beta_2'b_2'\alpha_2'a_2')(-)^{\alpha_2'+\beta_2'-\alpha_4}],\end{aligned} \tag{A2}$$

$$\langle 0|(P_{\beta_2}(nn;b_2)P_{\alpha_2}(pp;a_2))_{\alpha_4}(P^{\dagger}_{\alpha_2'}(pn;a_2')P^{\dagger}_{\beta_2'}(pn;b_2'))_{\alpha_4}|0\rangle=-\sum_{ijkl}B(ijkl;\alpha_2a_2\beta_2b_2\alpha_2'a_2'\beta_2'b_2'), \tag{A3}$$

where

$$\begin{aligned}A(ijkl;\alpha_2a_2\beta_2b_2\alpha_2'a_2'\beta_2'b_2')\equiv\hat{\alpha}_2\hat{\beta}_2\hat{\alpha}_2'\hat{\beta}_2'\begin{bmatrix}i&j&\alpha_2\\l&k&\beta_2\\\alpha_2'&\beta_2'&\alpha_4\end{bmatrix}(-)^{k+l-\beta_2+k+j-\beta_2'}X^{*}_{pn}(ij;\alpha_2a_2)X^{*}_{pn}(kl;\beta_2b_2)\\\times X_{pn}(il;\alpha_2'a_2')X_{pn}(kj;\beta_2'b_2'),\end{aligned} \tag{A4}$$

$$B(ijkl;\alpha_2a_2\beta_2b_2\alpha_2'a_2'\beta_2'b_2')\equiv\hat{\alpha}_2\hat{\beta}_2\hat{\alpha}_2'\hat{\beta}_2'\begin{bmatrix}i&j&\alpha_2\\k&l&\beta_2\\\alpha_2'&\beta_2'&\alpha_4\end{bmatrix}\overline{X}^{*}_{pp}(ij;\alpha_2a_2)\Delta_{ij}\overline{X}^{*}_{nn}(kl;\beta_2b_2)\Delta_{kl}X_{pn}(ik;\alpha_2'a_2')X_{pn}(jl;\beta_2'b_2'), \tag{A5}$$

with the following notation:

$$\overline{X}_{\tau\tau}(ij;\alpha_2a_2)\equiv\begin{pmatrix}X_{\tau\tau}(ij;\alpha_2a_2), & i\leqslant j\\(-)^{i+j+1+\alpha_2}X_{\tau\tau}(ji;\alpha_2a_2), & i>j\end{pmatrix}. \tag{A6}$$

## APPENDIX B: DIAGONALIZATION PROCEDURE IN THE NONORTHONORMAL BASIS

Let us introduce the following short-hand notations:

$$(\alpha_2a_2\beta_2b_2)\equiv i,\quad(\alpha_2'a_2'\beta_2'b_2')\equiv k,\quad(\alpha_4a_4)\equiv n. \tag{B1}$$

The expansion of the four-particle state $|n\rangle$ in terms of the nonorthonormal system of states $|k\rangle$, given by Eq. (2.9), with the above notation has the following form:

$$|n\rangle=\sum_k|k\rangle X_{kn}, \tag{B2}$$

and one can write the system of equations (2.11) as

$$\sum_k\langle i|H|k\rangle X_{kn}=E_n\sum_k\langle i|k\rangle X_{kn}. \tag{B3}$$

It can be solved by using the eigenstates of the Hermitian metric matrix $\langle i|k\rangle$:

$$\sum_k\langle i|k\rangle Y_{kj}=D_jY_{ij},\quad\sum_kY^{\dagger}_{ik}Y_{kj}=\delta_{ij}. \tag{B4}$$

Using the following orthonormal system of functions by excluding spurious eigenmodes with $D_i\approx0$,

$$|i\rangle = \sum_k |k\rangle \frac{Y_{ki}}{\sqrt{D_i}}, \tag{B5}$$

one obtains a standard diagonalization problem

$$\sum_j (i|H|j) Z_{jn} = E_n Z_{in} \tag{B6}$$

for the Hermitian matrix

$$(i|H|j) \equiv \sum_{kl} \frac{Y^{\dagger}_{ik}}{\sqrt{D_i}} \langle k|H|l\rangle \frac{Y_{lj}}{\sqrt{D_j}}. \tag{B7}$$

The expansion coefficients of the initial nonorthonormal basis $X_{kn}$ are given by

$$X_{kn} = \sum_i Y_{ki} \frac{1}{\sqrt{D_i}} Z_{in}. \tag{B8}$$


[1] G. Gamow, Z. Phys. **51**, 204 (1928).
[2] I. Tonozuka and A. Arima, Nucl. Phys. **A323**, 45 (1979).
[3] T. Fliessbach and S. Okabe, Z. Phys. A **320**, 289 (1985).
[4] F. A. Janouch and R. J. Liotta, Phys. Rev. C **27**, 896 (1983).
[5] G. Dodig-Crnkovic, F. A. Janouch, R. J. Liotta, and Z. Xiaolin, Phys. Scr. **37**, 523 (1988).
[6] S. M. Lenzi, O. Dragun, E. E. Maqueda, R. J. Liotta, and T. Vertse, Phys. Rev. C **48**, 1463 (1993).
[7] J. Dobaczewski, W. Nazarewicz, T. R. Werner, J. F. Berger, C. R. Chinn, and J. Decharge, Phys. Rev. C **53**, 2809 (1996).
[8] K. Varga, R. G. Lovas, and R. J. Liotta, Nucl. Phys. **A550**, 421 (1992).
[9] D. S. Delion, A. Insolia, and R. J. Liotta, Phys. Rev. C **54**, 292 (1996).
[10] T. Berggren, Nucl. Phys. **A109**, 265 (1968).
[11] T. Vertse, P. Curuchet, O. Civitarese, L. S. Ferreira, and R. J. Liotta, Phys. Rev. C **37**, 876 (1988).
[12] P. Curuchet, T. Vertse, and R. J. Liotta, Phys. Rev. C **39**, 1020 (1989).
[13] T. Vertse, R. J. Liotta, and E. Maglione, Nucl. Phys. **A584**, 13 (1995).
[14] E. Maglione, L. S. Fereira, and R. J. Liotta, Phys. Rev. Lett. **81**, 538 (1998).
[15] P.-H. Heenen, Nucl. Phys. **A272**, 399 (1976).
[16] N. Takigawa and S. Y. Lee, Nucl. Phys. **A292**, 173 (1977).
[17] P. Manngård, Ph.D. thesis, Åbo Akademi, Åbo, 1996.
[18] A. R. Barnett and J. S. Lilley, Phys. Rev. C **9**, 2010 (1974).
[19] P. Schuck, R. Wittman, and P. Ring, Lett. Nuovo Cimento **17**, 107 (1976).
[20] R. J. Liotta and C. Pomar, Nucl. Phys. **A362**, 137 (1981); **A382**, 1 (1982).
[21] G. Dodig-Crnkovic, F. A. Janouch, R. J. Liotta, and L. J. Sibanda, Nucl. Phys. **A444**, 419 (1985).
[22] G. Dodig-Crnkovic, F. A. Janouch, and R. J. Liotta, Nucl. Phys. **A501**, 533 (1989).
[23] H. J. Mang, Annu. Rev. Nucl. Sci. **14**, 1 (1964).
[24] B. F. Bayman and A. Kalio, Phys. Rev. **156**, 1121 (1967).
[25] B. F. Bayman, S. M. Lenzi, and E. E. Maqueda, Phys. Rev. C **41**, 109 (1990).
[26] S. Cwiok, J. Dudek, W. Nazarewicz, J. Skalski, and T. Werner, Comput. Phys. Commun. **46**, 379 (1987).
[27] T. Vertse, K. F. Pal, and Z. Balogh, Comput. Phys. Commun. **27**, 309 (1982).
[28] P. J. Brussaard and P. W. M. Glaudemans, *Shell-Model Applications in Nuclear Spectroscopy* (North-Holland, Amsterdam, 1977).
[29] D. Strottman, Phys. Rev. C **20**, 1150 (1979).
[30] R. Blendowske, T. Fliessbach, and H. Walliser, Nucl. Phys. **A464**, 75 (1987).
[31] R. B. Firestone, V. S. Shirley, S. Y. F. Chu, C. M. Baglin, and J. Zipkin, *Table of Isotopes*, CD-ROM, Eighth Edition, Version 1.0 (Wiley-Interscience, New York, 1996).
[32] E. Browne, Nucl. Data Sheets **65**, 209 (1992).